
THEORY
OF RADIO CIRCUITS

Design and Analysis of Complimentary Split Ring Resonator Backed Microstrip Transmission Line Using Equivalent Circuit Model¹

P. Garg^{a, *} and P. Jain^{a, **}

^a*Department of Electronics and Communication Engineering, Delhi Technological University, Shahbad Daultapur, New Delhi, 110042 India*

^{*}*e-mail: priyankagarg_phd2k16@dtu.ac.in*

^{**}*e-mail: priyankajain@dtu.ac.in*

Received July 29, 2018

Abstract—This article presents a compact, low-profile Band-Stop Filter (BSF) designed using Complimentary Split Ring Resonator (CSRR). An equivalent circuit model is also presented along with the simplified mathematical approach to extract the parameters of the circuit model. This paper also presents the effect of variation in the dimensions of split rings on characteristics of BSF. The proposed BSF has a compact size of $27 \times 20 \text{ mm}^2$ designed on FR-4 substrate with dielectric constant (ϵ_r) 4.3. The filter provides complete suppression of the band at 2.4 GHz. The design and circuit analysis of this metamaterial based filter is presented in terms of reflection coefficient, transmission coefficient and impedance curve.

Keywords: Bandstop filter (BSF), metamaterial, complementary split ring resonator (CSRR), microstrip line, resonator

DOI: 10.1134/S1064226918120069

INTRODUCTION

Bandstop filters form an essential element in various RF, microwave and other communication systems for suppressing undesired frequency bands. Various band-stop filters have been proposed using planar technology [1, 2]. Although at some point, the design suffers from the drawback of large dimensions, use of metamaterials in such cases has proven to exhibit an exceptional reduction in dimensions.

Metamaterials are artificially engineered structures that provide extraordinary characteristics such as negative permittivity ϵ_r and permeability μ_r . Split ring resonators (SRR) have been shown to exhibit negative permeability around resonant frequency [3]. Complementary Split Ring Resonator (CSRR) is the counter image of SRR which shows negative permittivity for a particular band of frequencies [4]. CSRR etched on the ground plane at the back of a microstrip line is a well-known technique to realize filters. Such filters provide exceptional in-band and out-of-band performance. Liu et al. [5] presented a CSRR based high pass filter utilizing C-shaped coupling. An Open Complementary Split Ring Resonator (OCSRR) with 80% fractional bandwidth at central frequency 5 GHz is designed in [6]. A wideband bandpass filter with

CSRR loaded microstrip transmission line is presented by Kim et al. [7] utilizing Evolution Strategy (ES) method for parameter optimization.

In this paper, a compact sized bandstop filter utilizing Complementary Split Ring Resonator (CSRR) is proposed. The proposed filter is designed to suppress the 2.4 GHz frequency band. Such filters can be extensively used in communication systems to avoid interference of original signal with other signals which may lead to error in output. The main objective of this paper is to demonstrate a methodology for selection of suitable equivalent circuit arrangement based on simulated results of the filter i.e. transmission coefficient and impedance curve, in order to study the electrical behavior of the design. Bonache et al. [8] presented the extraction of an equivalent circuit model, however using the methodology presented in this paper; we have found that the number of lumped elements used can be reduced further. A stepwise simplified mathematical approach for parameter extraction of the equivalent circuit is also presented. All the design and circuit simulations are performed using Computer Simulation Tomography Microwave Studio (CST-MWS) [9] and Computer Simulation Tomography Design Studio (CST-DS) [10]. Finally, the design is fabricated and measured.

¹ The article is published in the original.

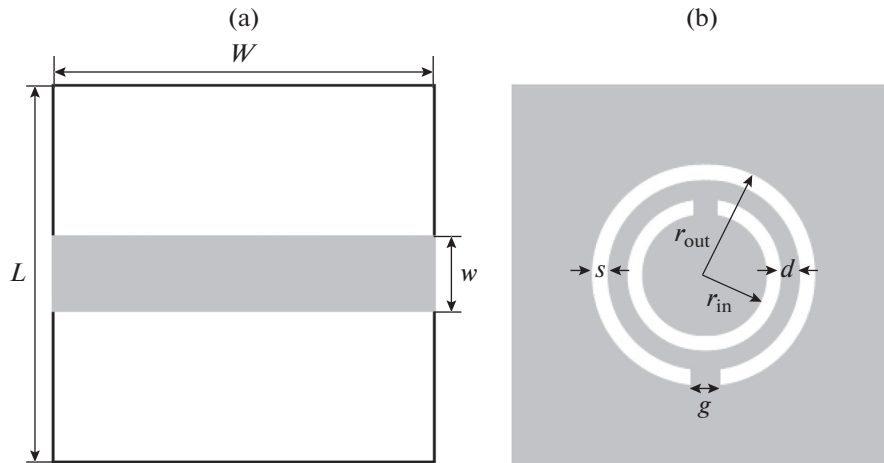


Fig. 1. Top microstrip line (a) and CSRR etched bottom ground plane (b).

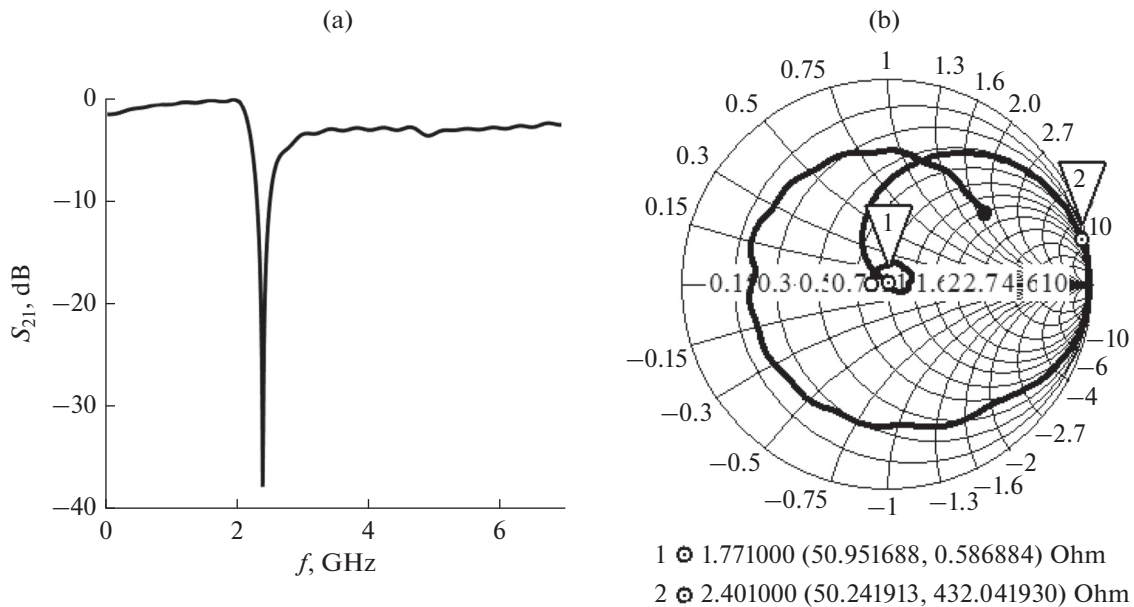


Fig. 2. The results of design simulation for frequency dependence of transmission coefficient (a) and impedance curve (b).

1. DESIGN AND CIRCUIT SIMULATION APPROACH

Figure 1 illustrates the geometry and dimensions of the proposed bandstop filter with a 50-Ω microstrip line on the top side and CSRR etched on the bottom ground plane. It is designed using an FR-4 dielectric substrate with relative permittivity (ϵ_r) 4.3, and thickness 1.6 mm. The proposed BSF has a compact size of only $27 \times 20 \text{ mm}^2$. The dimensions of the microstrip line are chosen to deliver 50-Ω characteristic impedance.

The design parameters of proposed bandstop filter are given as: $L = 20 \text{ mm}$, $W = 27 \text{ mm}$, $w = 3.1 \text{ mm}$, $r_{out} = 5 \text{ mm}$, $r_{in} = 2.85 \text{ mm}$, $g = 0.6 \text{ mm}$, $s = 0.7 \text{ mm}$ and $d = 0.75 \text{ mm}$.

In an SRR, each ring can be modeled as an inductor and the gap between the rings can be modeled as a capacitor. CSRR, being the dual of SRR, shows a complementary effect where the inductance is substituted by the capacitance of the disk and the gap capacitance is substituted by inductance between the slotted rings [11].

The circuit equivalent of the proposed BSF can be realized by using the transmission coefficient S_{21} and impedance characteristics, as shown in Figs. 2a, 2b respectively, obtained after design simulation. Since, the impedance curve shows inductive effect below resonant frequency and capacitive effect above it, so it is concluded that the circuit must contain a parallel res-

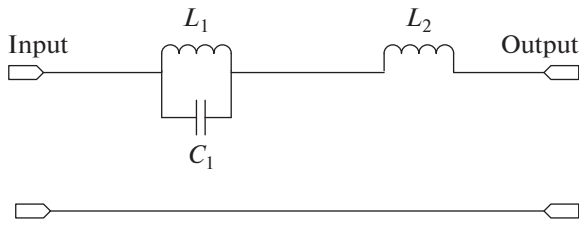


Fig. 3. Equivalent circuit of the proposed bandstop filter.

onant circuit. Further, S_{21} curve as shown in Fig. 2a, shows negative insertion loss (IL), given by,

$$IL = 10\log_{10} |S_{21}(f)|^2. \tag{1}$$

Thus, the circuit equivalent of the simulated bandstop filter is a series connected parallel resonant circuit. The proposed bandstop filter shows maximum transmission at 1.771 GHz and minimum transmission at 2.401 GHz. Figure 3 shows the equivalent circuit obtained on the basis of simulated results.

Consider f_1 be the maximum transmission frequency, f_2 be the minimum transmission frequency and f_3 be the frequency at which IL is 3 dB such that $f_1 < f_3 < f_2$. The value of f_3 is obtained at the intersection of reflection and transmission coefficient S_{11} and S_{21} respectively, since,

$$|S_{11}|^2 + |S_{21}|^2 = 1 \tag{2}$$

and at the intersection point, $S_{11} = S_{21}$. Thus, $S_{11} = 1/\sqrt{2}$, a point of 3 dB IL.

The stepwise parameter extraction method, considering the circuit to be lossless, is summarized below.

(i) At the resonance condition of the parallel LC circuit i.e. f_2 , S_{21} leads to zero. This gives the equation for C_1 in terms of L_1 and frequency f_2 .

(ii) At the resonance condition of the whole tank circuit i.e. f_1 , S_{11} leads to zero. This gives the relation for L_1 in terms of L_2 and frequencies f_1, f_2 .

(iii) Finally, at 3 dB IL with frequency f_3 , the third relation for L_2 in terms of frequency f_1, f_2 and f_3 is obtained.

The S -parameter matrix of the series connected parallel LC resonator is given by,

$$[S] = \begin{bmatrix} \frac{Y_0}{Y_0 + 2Y} & \frac{2Y}{Y_0 + 2Y} \\ \frac{2Y}{Y_0 + 2Y} & \frac{Y_0}{Y_0 + 2Y} \end{bmatrix},$$

where $Y_0 = 1/Z_0$, Z_0 is the characteristics impedance of the line which is 50-Ω and Y is the input admittance of the LC circuit.

The mathematical approach for parameter extraction using above steps is summarized below.

(i) Taking $S_{21} = 0$. Considering only parallel LC circuit (L_1, C_1), the input admittance is expressed as,

$$Y = \frac{1 - \omega^2 L_1 C_1}{j\omega L_1}. \tag{3}$$

From the S -parameter matrix,

$$S_{21} = \frac{2Y}{Y_0 + 2Y} = \frac{2 \left[\frac{1 - \omega_2^2 L_1 C_1}{j\omega_2 L_1} \right]}{Y_0 + 2 \left[\frac{1 - \omega_2^2 L_1 C_1}{j\omega_2 L_1} \right]} = 0, \tag{4}$$

$$1 - \omega_2^2 L_1 C_1 = 0. \tag{5}$$

On solving the above equation, we obtain,

$$C_1 = \frac{1}{4\pi^2 f_2^2 L_1}. \tag{6}$$

(ii) Equating S_{11} to zero,

$$S_{11} = \frac{Y_0}{Y_0 + 2Y} = \frac{Z}{Z + 2Z_0} = 0. \tag{7}$$

Considering the input impedance of the overall tank circuit,

$$Z = \frac{j\omega_1 L_1}{1 - \omega_1^2 L_1 C_1} + j\omega_1 L_2. \tag{8}$$

Substituting the value of Z from Eq. (8) to Eq.(7), we obtain,

$$\frac{j\omega_1 L_1}{1 - \omega_1^2 L_1 C_1} + j\omega_1 L_2 = 0. \tag{9}$$

On solving, one can get,

$$L_1 + L_2 - \omega_1^2 L_1 L_2 C_1 = 0. \tag{10}$$

Substituting here the value of C_1 from Eq. (6), obtain

$$L_1 + L_2 - \frac{\omega_1^2}{\omega_2^2} L_2 = 0. \tag{11}$$

Solving for L_1 , we get

$$L_1 = L_2 \left[\frac{f_1^2}{f_2^2} - 1 \right] = 0. \tag{12}$$

(iii) Now, the condition for 3 dB IL is given as,

$$|S_{21}| = \frac{2Y}{Y_0 + 2Y} = \frac{2Z_0}{Z + 2Z_0} = \frac{1}{\sqrt{2}}, \tag{13}$$

$$\frac{2Z_0}{\sqrt{\left[\frac{j\omega_3 L_1}{1 - \omega_3^2 L_1 C_1} + j\omega_3 L_2 \right]^2 + 4Z_0^2}} = \frac{1}{\sqrt{2}}. \tag{14}$$

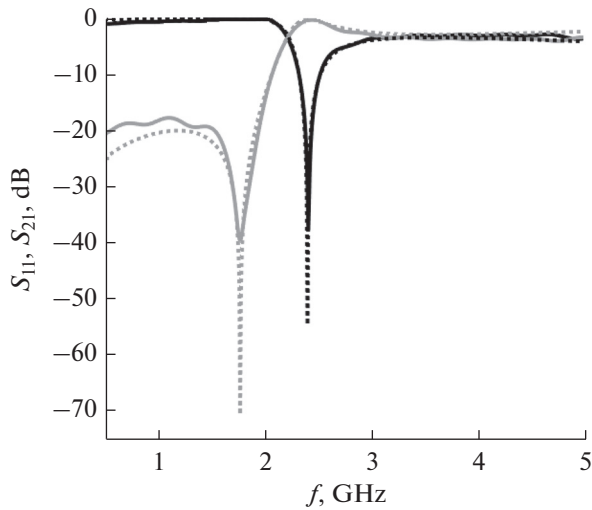


Fig. 4. Frequency dependences of reflection coefficients S_{11} (grey curves) and transmission coefficient S_{21} (black curves) obtained by design (solid curves) and circuit (dotted curves) simulation.

Now, on substituting the value of C_1 from Eq. (6) in Eq. (14) and solving, we get,

$$2Z_0 \left(1 - \frac{f_3^2}{f_2^2} \right) = \omega_3 \left[L_1 + L_2 \left(1 - \frac{f_3^2}{f_2^2} \right) \right]. \quad (15)$$

Substituting the value of L_1 from Eq. (12) in Eq. (15) and solving, we obtain,

$$L_2 = \frac{Z_0 (f_2^2 - f_3^2)}{\pi f_3 (f_1^2 - f_3^2)}. \quad (16)$$

2. RESULTS AND DISCUSSIONS

From the results obtained after simulating the BSF design, we get $f_1 = 1.771$ GHz, $f_2 = 2.401$ GHz, $f_3 = 2.217$ GHz. Substituting all these values into Eqs. (6), (12), (16), we obtain the values of circuit parameters L_1, C_1, L_2 as 1.563 nH, 2.81 pF and -3.429 nH respectively. Using the values of L_1, C_1, L_2 , the equivalent circuit of BSF is designed and simulated in CST design studio and results are obtained. Figure 4 shows the simulated reflection and transmission coefficient of the CSRR based BPF comparative to that of its circuit equivalent. Also, Figs. 5a and 5b simultaneously show the impedance curve of simulated design and circuit. Little mismatch in the impedance may be due to the presence of losses in the design. Both the results show that the circuit is a close approximation of the proposed BSF.

Now, it is important to note that the value of inductance L_2 is a negative quantity. It can be explained as the presence of an equivalent capacitance, say C'_2 [12]

$$X_L = -j\omega L_2, \quad (17)$$

where negative sign indicates the negative nature of inductance L_2 . Further rearranging the Eq. (17), we get,

$$X_L = \frac{1}{j\omega \left(\frac{1}{\omega^2 L_2} \right)}. \quad (18)$$

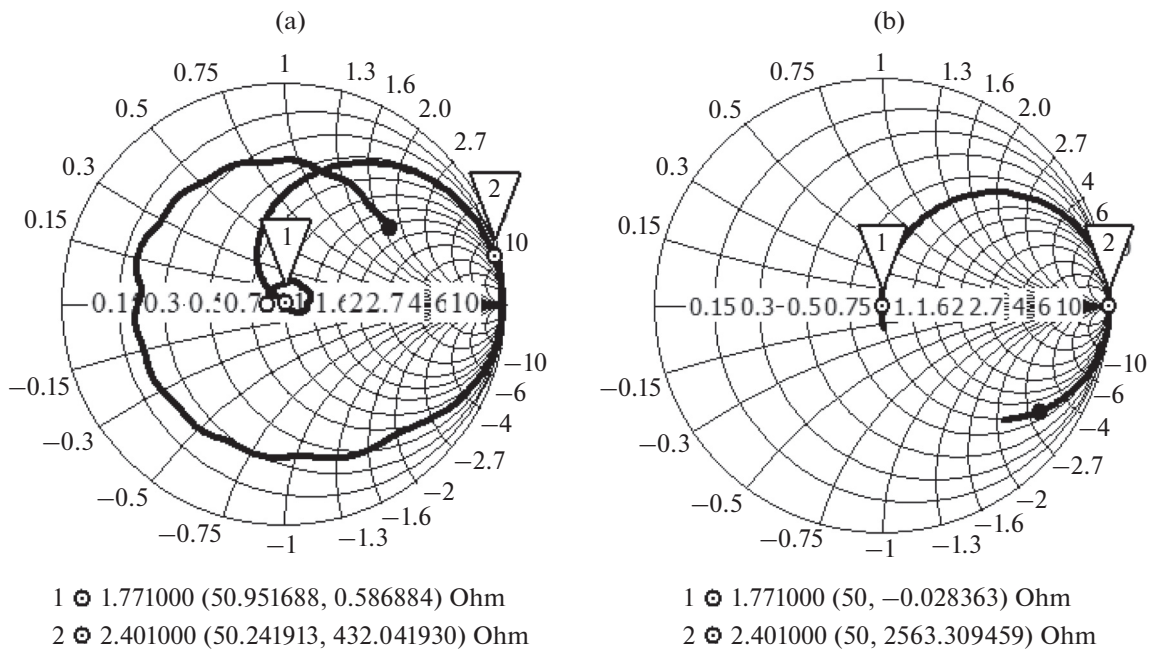


Fig. 5. Impedance curves obtained by design (a) and circuit (b) simulations.

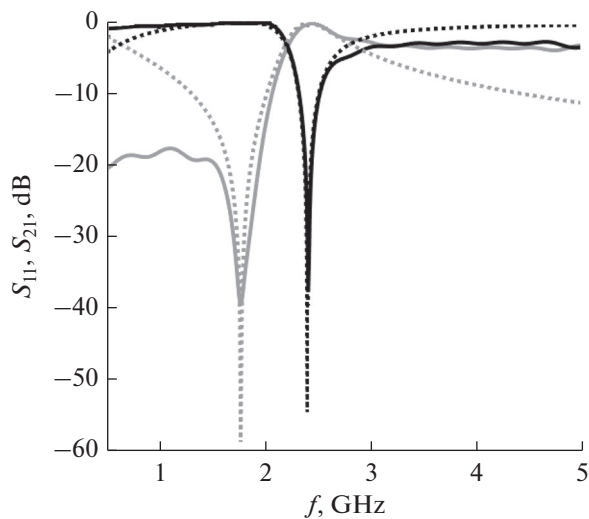


Fig. 6. Frequency dependences of reflection coefficients S_{11} (grey curves) and transmission coefficient S_{21} (black curves) obtained by design (solid curves) and circuit (dotted curves) simulation after replacing inductor L_2 shown in Fig. 3 by capacitor C'_2 .

Thus,

$$C'_2 = \frac{1}{\omega^2 L_2} \tag{19}$$

Since there is two resonance phenomenon observed in the design, one is the parallel resonance occurring at f_2 and the other is the weak series resonance occurring at lower frequency f_1 . At f_2 , resonance is due to the parallel resonant circuit L_1 and C_1 . At lower frequency, the parallel resonant circuit behaves as an inductor, say L'_1 . On connecting C'_2 in series with L'_1 we get a weak series resonance at f_1 .

From Eq. (19), C'_2 at frequency f_1 is obtained as 2.35 pF. The simulated results after replacing the neg-

ative inductance L_2 by the equivalent positive capacitance C'_2 is shown in Fig. 6.

3. PARAMETRIC ANALYSIS

Three dimensions are selected for parametric analysis that exhibit major variation in the characteristics of BSF. First one is the radius of the split rings. Figure 7a shows the variation in r_{out} keeping the dimensions s , d and g unchanged. It was observed that as r_{out} is increased from 4 mm to 6 mm, the resonant frequency shifts towards the lower side.

The second dimension for parametric analysis is the distance between the two rings d . Figure 7b shows variation in d keeping other parameters unchanged. As the parameter d is increased from 0.25 to 1.25 mm, the frequency again shifts to lower values.

Finally, variation in the split gap g is performed. Figure 7c shows as the split gap of the rings is increased from 0.2 to 1.8 mm, the frequency shifts towards higher values. Thus, suitable dimensions of the CSRR can be selected to obtain the desired resonant frequency as per the required specification.

4. EXPERIMENTAL RESULTS AND DISCUSSIONS

Figure 8 shows the fabricated bandstop filter showing a microstrip transmission line on top and CSRR etched on the bottom ground plane. Keysight N9914A vector network analyzer is used to carry out the measurements of various parameters of the fabricated CSRR based BSF such as reflection coefficient, transmission coefficient, and 3-dB bandwidth. Figure 9 shows the S -parameters as observed on the Keysight N9914A vector network analyzer. Figure 10 simultaneously shows the measured; design simulated and circuit simulated values of S -parameters of the proposed BSF. The measured results show a 3-dB stop-band from 2.113 to 3.088 GHz giving a 3-dB band-

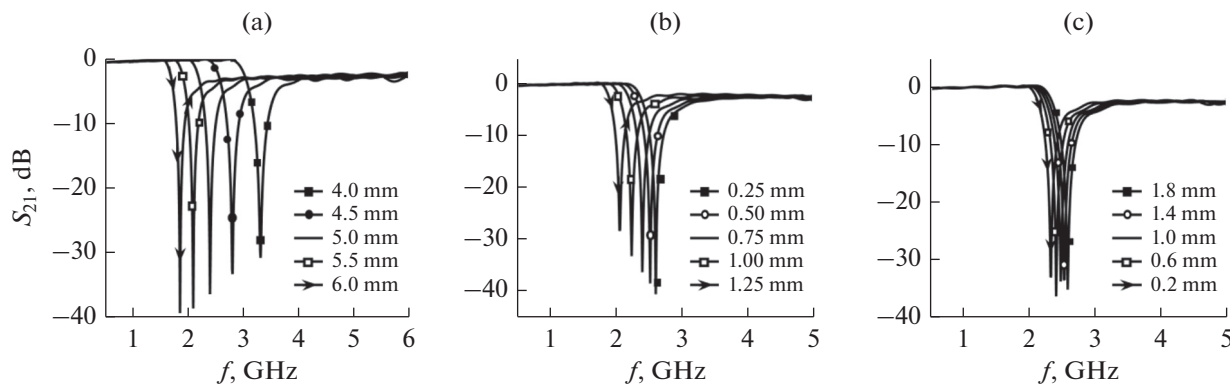


Fig. 7. Parametric analysis of frequency dependence of transmission coefficient S_{21} : r_{out} (a), d (b) and g (c).

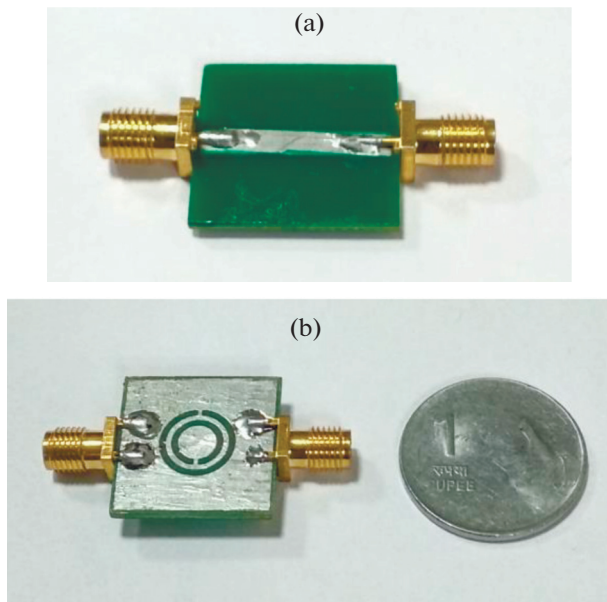


Fig. 8. Fabricated BSF: (a) top view, (b) bottom view. For comparison: the diameter of 1 Indian Rupee coin is approximately 22 mm.

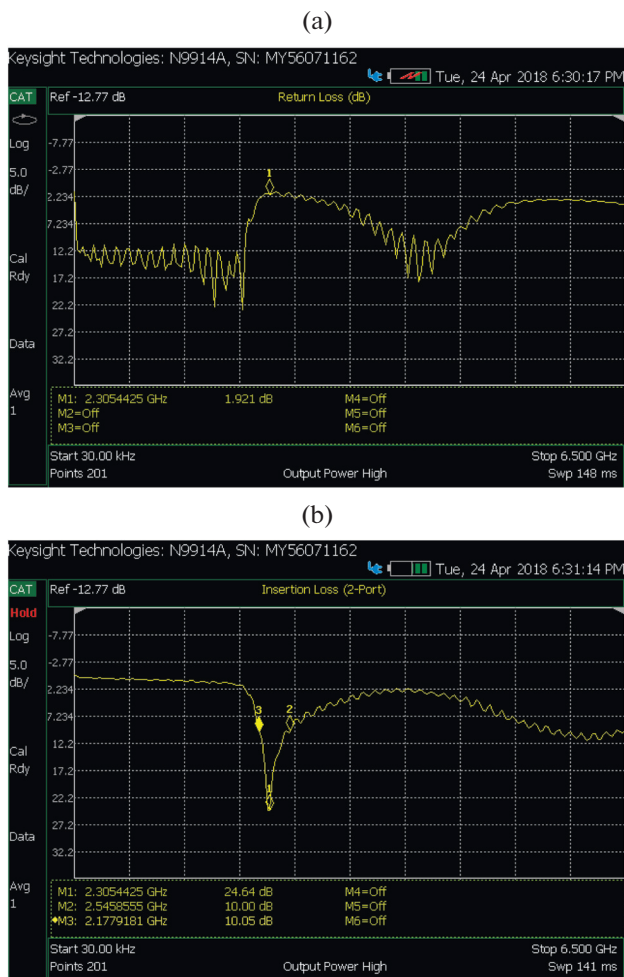


Fig. 9. Snapshots of results on Keysight N9914A vector network analyzer: (a) return loss, (b) insertion loss.

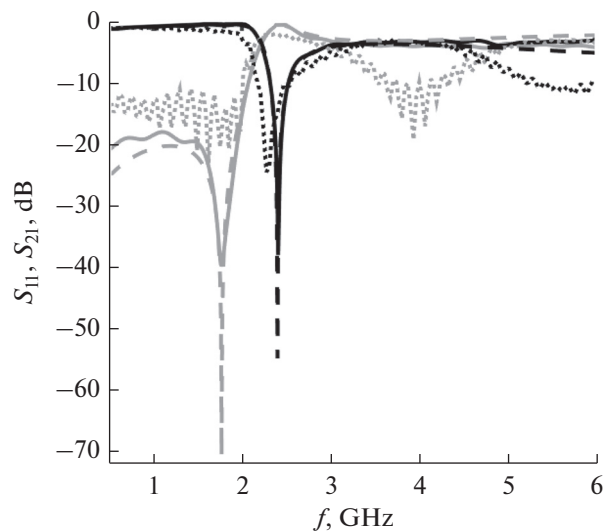


Fig. 10. Frequency dependences of reflection and transmission coefficients of proposed BSF: S_{11} (grey curves) and S_{21} (black curves). Solid curves are obtained by design simulation, dashed curves—by circuit simulation, dotted curves—measured values.

width of 0.975 GHz. The occurrence of ripples in the measured results may be due cable losses. The measured results match well with the simulated results.

CONCLUSIONS

A complementary split ring resonator based band-stop filter has been designed and simulated. A stop band at the vicinity of 2.4 GHz is obtained. Based on the simulated results, the circuit arrangement is defined to be a series connected parallel resonant circuit followed by a series connected inductor. The simplified mathematical approach is described in detail to obtain the lumped circuit parameters. Only three lumped components are used to define the circuit model, thus reducing the circuit complexity. Furthermore, the parametric variation of the split rings is analyzed which displays frequency tuning capability by varying the dimensions of split rings. Finally, the filter is fabricated and measured to show fair agreement with the simulated results. The proposed bandstop filter shows good lower passband performance. The high-frequency passband shows large reflections which may be improved further.

REFERENCES

1. R. Habibi, C. Ghobadi, J. Nourinia, et al., *Electron. Lett.* **48**, 1483 (2012).
2. D. La, Y. Lu, S. Sun, et al., *Microwave and Opt. Technol. Lett.* **53**, 433 (2010).
3. J. B. Pendry, A. J. Holden, D. J. Robbins, et al., *IEEE Trans. Microwave Theory Tech.* **47**, 2075 (1999).

4. F. Falcone, T. Lopetegi, J. D. Baena, et al., *IEEE Microwave and Wireless Compon. Lett.* **14**, 280 (2004).
5. J. C. Liu, D. S. Shu, B. H. Zeng, et al., *IET Microwaves, Antennas and Propag.* **2**, 622 (2008).
6. A. Velez, F. Aznar, J. Bonache, et al., *IEEE Microwave and Wireless Compon. Lett.* **19**, 197 (2009).
7. K. T. Kim, J. H. Ko, K. Choi, et al., *IEEE Trans. Magnetics* **48**, 811 (2012).
8. J. Bonache, M. Gil, I. Gil, et al., *IEEE Microwave and Wireless Compon. Lett.* **16**, 543 (2006).
9. Computer Simulation Technology Microwave Studio (CST MWS). Available at <http://www.cst.com>.
10. Computer Simulation Technology Design Studio (CST DS). Available at <http://www.cst.com>.
11. J. D. Baena, J. Bonache, F. Martn, et al., *IEEE Trans. Microwave Theory Tech.* **53**, 1151 (2005).
12. A. Abdel-Rahman, A. K. Verma, A. Boutejdar, et al., *IEEE Microwave and Wireless Compon. Lett.* **14**, 136 (2004).